CHEMISTRY
A EUROPEAN JOURNAL

COMMUNICATION

DOI: 10.1002/chem.201203687

Robust Phosphorescent Platinum(II) Complexes Containing Tetradentate O^N^C^N Ligands: Excimeric Excited State and Application in Organic White-Light-Emitting Diodes

Steven C. F. Kui, Pui Keong Chow, Glenna So Ming Tong, Shiu-Lun Lai, Gang Cheng, Chi-Chung Kwok, Kam-Hung Low, Man Ying Ko, and Chi-Ming Che*[a]

Intra- and intermolecular metal–metal and ligand–ligand interactions are important characteristic features of platinum(II) complexes that have chelating C and/or N atom donor ligands;[1–3] such complexes could be harnessed for self-assembly of nanostructured materials[4] and used for developing luminescent sensors of biological targets.[5] These intramolecular/intermolecular interactions give rise to low-energy metal–metal-to-ligand charge transfer (MMLCT) and/or π(ligand)···π(ligand) excimeric excited states leading to red-shifts in both absorption and emission energies of oligomers from the corresponding monomeric counterparts.[1–3] In this area, cyclometalated platinum(II) complexes have been extensively studied as they exhibit dual phosphorescence in the high-energy (bluish green) and low-energy (reddish orange) spectral regions. These two types of emission bands are often attributed to monomeric and excimeric emissions, respectively. The electronic structure of the excimeric excited states of Pt^{II} complexes (Figure 1), however, remains elusive. More than 20 years ago, Miskowski et al. suggested that the low-energy excimer emission is ascribed to 1) metal–metal-to-ligand charge transfer (^{3}MMLCT) for which upon excitation, there is an enhanced Pt···Pt interaction with concomitant shortening of the Pt···Pt distance or 2) transitions involving π···π interactions between aromatic ligands of interplanar separation <3.5 Å.[6] Brédas and Kim lately reported DFT/TDDFT calculations on FPt1 (FPt1 = [2-(4′,6′-difluorophenyl)pyridinato-*N*,*C*$^{2'}$](2,4-pentanedionato)platinum(II)) and their conclusion is in concordance with the proposal of Miskowski and co-workers, namely, an excimer is formed through the cooperative effect of both Pt···Pt and interligand π···π interactions.[7] On the other hand, Forrest and D'Andrade, based on the photoluminescent and electroluminescent studies on neat films of FPt1, proposed that the triplet excimer is formed through interactions between a monomer triplet exciton and a monomer ground state; the stabilization of the excimer is accounted for by a configuration interaction between exciton resonance and charge-transfer resonance states.[8] Recently, Kalinowski et al. made a similar conclusion on the formation of excimers from [Pt(N^C^N)Cl] (N^C^N = 1,3-di(2-pyridyl)benzene and it's derivatives).[9]

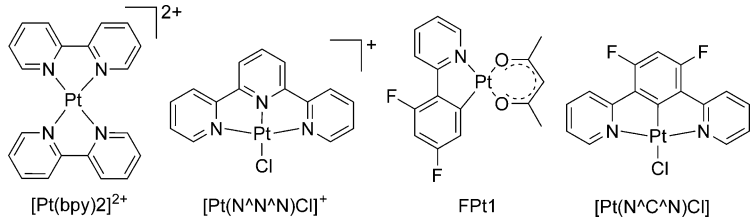

Figure 1. Chemical structures of selected Pt^{II} complexes showing low-energy excimeric emissions.

Herein, we report a new series of cyclometalated platinum(II) complexes supported by a rigid tetradentate ligand O^N^C^N (O^N^C^N = 5,5-dibutyl-2-(3-(pyridin-2-yl)-phenyl)-5*H*-indeno[1,2-*b*]pyridin-9-olate and it's derivatives; **1–5** Scheme 1). The substitution pattern of the O^N^C^N ligand was found to significantly affect the properties of the excimeric emissive excited states. High-efficiency white organic light-emitting diodes (WOLEDs) [peak current effi-

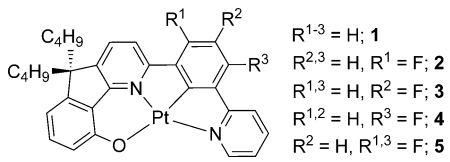

Scheme 1. Chemical structure of complexes **1–5**.

[a] Dr. S. C. F. Kui,[+] P. K. Chow,[+] Dr. G. S. M. Tong,[+] Dr. S.-L. Lai, Dr. G. Cheng, Dr. C.-C. Kwok, Dr. K.-H. Low, M. Y. Ko, Prof. C.-M. Che
State Key Laboratory of Synthetic Chemistry
Department of Chemistry
HKU-CAS Joint Laboratory on New Materials and
The University of Hong Kong, Pokfulam Road
Hong Kong (P. R. China)
Fax: (+852) 2915-5176
E-mail: cmche@hku.hk

[+] These authors contributed equally to this work.

Supporting information for this article is available on the WWW under http://dx.doi.org/10.1002/chem.201203687.

ciency ($\eta_{L(max)}$) = 71.0 cd A^{-1}, power efficiency ($\eta_{p(max)}$) = 55.8 lm W^{-1}, external quantum efficiency ($\eta_{Ext(max)}$) = 16.5 %, CIE = 0.33, 0.42, CRI = 77] and white polymer light-emitting diodes (WPLEDs) ($\eta_{L(max)}$ = 17.0 cd A^{-1}, $\eta_{p(max)}$ = 9.1 lm W^{-1}, $\eta_{Ext(max)}$ = 9.7 %, CIE = 0.43, 0.45, CRI = 78) have been fabricated using a simple device architecture and with **5** as a single emissive dopant.

Platinum(II) complexes bearing symmetric tetradentate chelating ligands, such as octaethylporphyrin (OEP),[10] bis(2′-phenol)bipyridine (N_2O_2),[11] Schiff base (Salphen),[12] bis(pyrrole)diimine (Prtmen),[13] *N*,*N*-di(2-phenylpyrid-6-yl)aniline (C^N^N^C)[14] and bis(*N*-heterocyclic carbene) (tetra-NHC),[15] are good phosphorescent emitters. The unsymmetric Pt^{II} complexes of O^N^C^N ligands in this work are highly emissive (ϕ up to 0.93), thermally stable (T_d > 400 °C), and could be obtained in high purity by sublimation at about 290 °C under 4×10^{-5} Torr. They were prepared by a procedure that gave high product yields (up to 80 %). The characterization data of **1**–**5** and X-ray crystallographic data of **1**, **3**, and **5** are given in the Supporting Information along with the synthetic procedures.[16] A perspective view of **5** is depicted in Figure 2.

The [(O^N^C^N)Pt] motifs of **1**, **3**, and **5** are virtually planar with the O1-N2-C11-N1 torsion angles being 0.13, 0.69, and 0.17°, respectively. Orthogonal packing is observed in the unit cells of **1**, **3**, and **5** with short intermolecular C–H···π distances in the range of 2.67–2.81 Å between the H atoms of the *n*-butyl chain and the O^N^C^N moiety. In the crystal structures of **1**, **3**, and **5**, the molecules in each case are orientated in pairs with a head-to-tail arrangement. Extensive intermolecular π···π interactions (π···π distances = 3.48–3.51 Å) are observed, but the intermolecular Pt···Pt distances are greater than 4.5 Å, revealing no intermolecular Pt···Pt interactions.

The absorption spectra of **1**–**5** in CH_2Cl_2 (Table 1) display intense bands at wavelengths below 300 nm (ε in the range 2.1–4.8 × 10^4 dm^3 mol^{-1} cm^{-1}) and moderate intense absorption bands at 400–435 nm (ε in the range 5300–9600 dm^3 mol^{-1} cm^{-1}) with weak absorption tails at > 460 nm (ε in the range 400–600 dm^3 mol^{-1} cm^{-1}). These absorptions

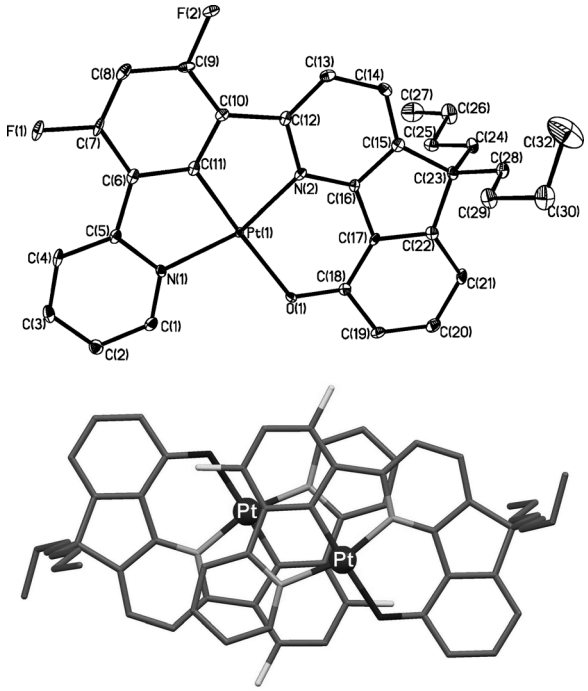

Figure 2. Perspective view (top) and molecular packing (bottom) of complex **5** (all hydrogen atoms are omitted for clarity).

are assigned to intraligand ^{1}π–π* transitions of the O^N^C^N ligands and mixed ^{1}MLCT/^{1}π–π* transitions (MLCT = metal-to-ligand charge transfer), respectively.

Complexes **1**–**5** show vibronic structured emission bands at λ_{max} in the range 480–520 nm with emission quantum yields of 0.72–0.93 and emission lifetimes (τ) in the microsecond time regime in degassed CH_2Cl_2 (Table 1). As the vibrational spacings of 1300–1400 cm^{-1} correspond to the C=N/C=C stretching frequencies of the O^N^C^N ligands, the emissions are attributed to come from triplet excited states with predominant ligand character.

Upon increase in complex concentration, a low-energy emission is observed with **2**, **4**, or **5** in CH_2Cl_2. As depicted in Figure 3, the high-energy vibronic structured emission at

Table 1. Physical data of complexes **1**–**5**.

	UV/Vis absorption[a] λ_{max} [nm] (ε [×10^4 mol^{-1} dm^3 cm^{-1}])	Emission Solution [a] λ_{max}[nm] (τ [μs])	Quantum yield[b]	K_q[c] [mol^{-1}dm^{3}s^{-1}]	HOMO[d] [eV]	LUMO[d] [eV]	Electro-chemical bandgap [eV][d]	T_d [°C]
1	254 (4.59), 280 (3.16), 354 (1.77), 390 (1.46), 426 (0.91)	485, 517, 557 (12.0)	0.72	5.4×10^8	−5.11	−2.62	2.49	414
2	254 (4.24), 261 (4.18), 290 (2.51), 352 (1.71), 388 (1.42), 429 (0.57)	488, 522 (28.0)	0.80	3.3×10^8	−5.17	−2.66	2.51	418
3	247 (3.72), 261 (3.43), 279 (2.67), 356 (1.52), 395 (1.15), 439 (0.70)	508, 543, 594 (11.0)	0.89	8.5×10^8	−5.12	−2.70	2.42	411
4	251 (4.82), 261 (4.55), 294 (2.07), 350 (1.83), 381(1.40), 424 (0.86)	488, 518 (13.2)	0.93	1.3×10^8	−5.15	−2.72	2.43	406
5	245 (4.58), 259 (4.45), 289 (2.65), 3.01 (1.86), 349 (1.78), 376 (1.35), 424 (0.66)	482, 512 (17.7)	0.75	1.2×10^9	−5.24	−2.71	2.53	432

[a] Determined in degassed CH_2Cl_2 (2×10^{-5} mol dm^{-3}). [b] Emission quantum yield was measured in degassed CH_2Cl_2 (2×10^{-5} mol dm^{-3}) by the optical dilute method with $[Ru(bpy)_3](PF_6)_2$ (bpy = 2,2′-bipyridine) in degassed CH_3CN as standard (ϕ_r = 0.062). [c] Self-quenching constant. [d] The HOMO and LUMO levels are estimated from onset potentials using $Cp_2Fe^{0/+}$ value of 4.8 eV below the vacuum level.

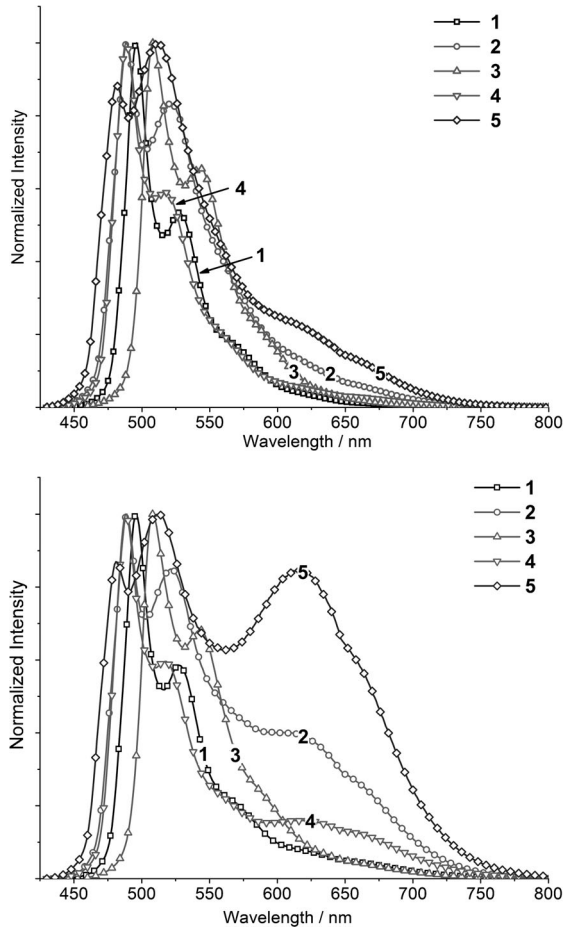

Figure 3. Emission spectra of **1**–**5** in CH_2Cl_2 (top: 2.0×10^{-5} mol dm^{-3}; bottom: 1.0×10^{-4} mol dm^{-3}).

480–520 nm decreases in intensity, while a low-energy emission band at about 620 nm develops as the complex concentration increases from 2×10^{-5} to 1×10^{-4} mol dm^{-3} (see Figure 3 and Figure S15 in the Supporting Information). As the excitation spectra for both the high- and low-energy emissions are the same and the absorption spectra of these three Pt^{II} complexes obey the Beer–Lambert law in the concentration range of 2×10^{-5} to 1×10^{-4} mol dm^{-3}, the low-energy emission in each of the three cases should not come from a ground-state dimer of the Pt^{II} complex with a close Pt···Pt contact. Instead, we attribute this finding to excimer emission. In contrast, both **1** and **3** display high-energy vibronic structured emission even at concentrations of 1×10^{-4} mol dm^{-3} (Figure 3). The details are given in Figure S14 in the Supporting Information.

DFT/TDDFT calculations were performed on complexes **3** and **5**. Two triplet excited states, labeled here as $^3MLCT_A$ and $^3MLCT_B$, have been located for both complexes. For $^3MLCT_A$, the transition is mainly localized on the phenyl and pyridyl rings of the O^N^C^N ligand, whereas for $^3MLCT_B$, the transition is localized mainly on the phenyl and the indenyl rings (see Figure 4 for the difference density plots for the two triplet excited states of **5**; similar plots

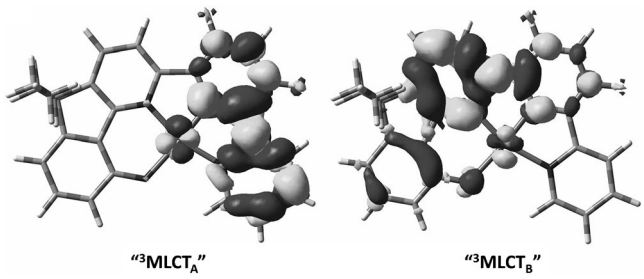

Figure 4. Difference density plots of $^3MLCT_A$ (left) and $^3MLCT_B$ (right) for complex **5**. Black: decrease in electron density; gray: increase in electron density.

were found for complex **3**, see the Supporting Information). In the case of **5**, these two triplet excited states are separated by about 0.18–0.24 eV in CH_2Cl_2, with $^3MLCT_B$ being lower in energy at their optimized geometries. The calculated emission energies for $^3MLCT_A$ and $^3MLCT_B$ are 564 and 593–642 nm, respectively.[17] On the other hand, for **3**, the two triplet excited states are quasi-degenerate in CH_2Cl_2, with $^3MLCT_A$ being 0.01–0.07 eV more stable than $^3MLCT_B$. The calculated emission energies for $^3MLCT_A$ and $^3MLCT_B$ are 586 and 555 nm, respectively. Thus, for **5**, two emission peaks are observed, while for **3**, the two emission peaks may coincide. We thus assign the high-energy emission peak of **5** at 480–520 nm to be derived from $^3MLCT_A$ and the accompanying low-energy emission peak at 620 nm to be coming from $^3MLCT_B$, whereas for **3**, the band at about 510 nm may possibly arise from both $^3MLCT_A$ and $^3MLCT_B$.

Conventionally, the low-energy emission that grows as the concentration increases is attributed to excimer formation. Here, we propose that the low-energy "excimer"-like emission of **5** at about 620 nm could be mainly attributed to emission from the $^3MLCT_B$ excited state localized on one [Pt(O^N^C^N)] motif. We have also performed calculations of the dimer of complex **5** to see if there is a triplet excited state that delocalizes over the two monomers and has similar emission energy as the low-energy emission at about 620 nm. It was found that the optimized triplet excited state of the dimer of **5** is localized on only one monomer and the nature is similar to $^3MLCT_B$ with emission energy calculated to be at approximately 640 nm (see Figure 5).

The strong excimer emission of **5** with high emission quantum yield even in dilute solution ($\times10^{-5}$ mol dm^{-3}) suggests the potential of using this complex as a single emitter for WOLEDs. Devices **A**–**F** were fabricated with a simple configuration of ITO/NPB (40 nm)/mCP:complex **5** (6–16%, 30 nm)/BAlq (40 nm)/LiF (0.5 nm)/Al (80 nm) [ITO = indium tin oxide; NPB = *N*,*N*′-diphenyl-*N*,*N*′-bis(1-naphthyl)-(1,1′-biphenyl)-4,4′-diamine; mCP = 1,3-bis(*N*-carbazolyl)benzene; BAlq = aluminum(III) bis(2-methyl-8-quinolinate)-4-phenylphenolate]. The electroluminescence (EL) spectra and CIE coordinates of devices **A**–**F** are depicted in Figures 6 and 7, respectively. Device **A** (6%, complex **5**) shows a warm white emission with CIE coordinates of (0.32, 0.43), $\eta_{L(max)}$ of 36.6 cd A^{-1}, $\eta_{p(max)}$ of 25.5 lm W^{-1}, and η_{Ext} of

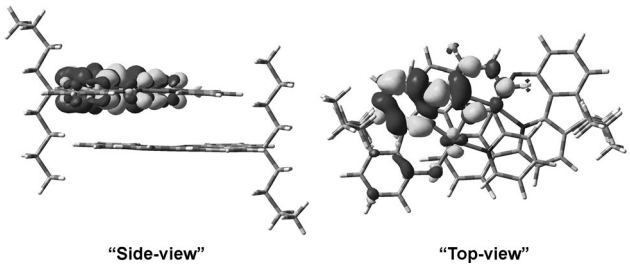

Figure 5. Difference density plots of the optimized triplet excited state of complex **5** dimer. Black: decrease in electron density; gray: increase in electron density.

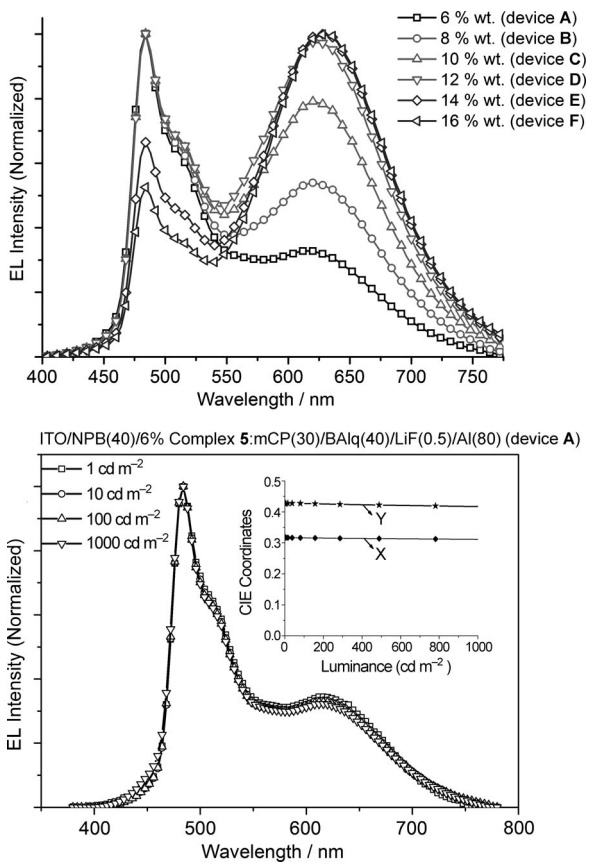

Figure 6. Top: EL spectra of devices **A**–**F** based on complex **5** with 6–16% dopant concentration at 100 cd m^{-2}. Bottom: EL spectra of device **A** at different luminance (inset: a plot of CIE against luminance).

17.7% (Table S16 in the Supporting Information). The EL spectra and CIE coordinates of device **A** are insensitive to luminance (1–1000 cd m^{-2}) (Figure 6).

To further improve the device efficiency, an electron blocking layer (EBL) was inserted between the hole-transport layer and the emissive layer to give devices **G**–**J** (ITO/NPB (40 nm)/EBL (10 nm; **G**: mCP or **H**: TCTA or **I**: [Ir(ppz)$_3$]; **J**: NPB)/mCP:complex **5** (6%, 20 nm)/BAlq (40 nm)/LiF (0.5 nm)/Al (80 nm) [TCTA = 4,4′,4″-tris-(*N*-carbazolyl)triphenlyamine]. The CIE coordinates of devices

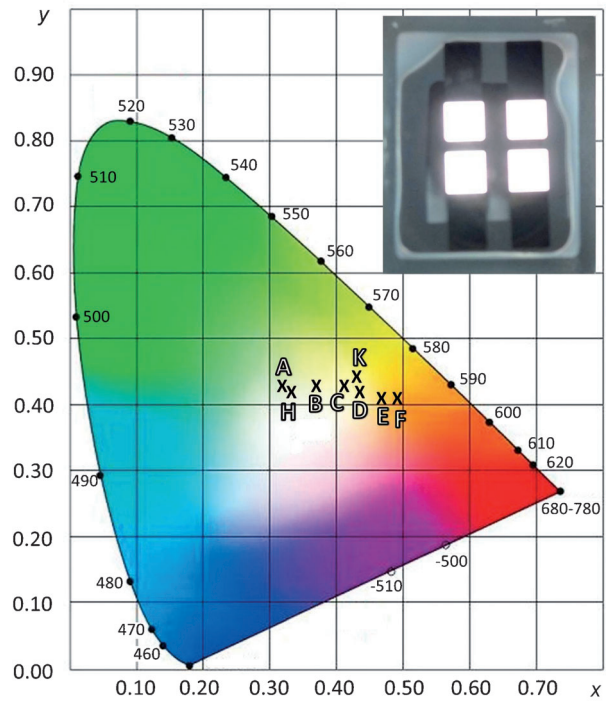

Figure 7. CIE 1931 chromaticity coordinates of devices **A**–**F**, **H**, and **K**; the inset shows a photograph of device **H** at 9 V.

G–**J** were kept to be the same as device **A** at around (0.32, 0.43) with CRI about 77. The turn-on voltages of devices **G**–**J** were found to be below 4 V. Values for the parameters $\eta_{L(max)}$ of 71.0 cd A^{-1}, $\eta_{p(max)}$ of 55.8 lm W^{-1}, and η_{Ext} of 16.5% were obtained with device **H** (Table S16 in the Supporting Information). The performance of device **H** is comparable with the WOLED fabricated by Jabbour et al. and Williams et al. by using FPt1[18] and [Pt(N^C^N)Cl][19–20] (Figure 1), respectively, as single emissive dopant, which have the an η_{Ext} of about 18% and $\eta_{p(max)}$ of about 30 lm W^{-1}.

To demonstrate further application of these complexes, white polymer light-emitting devices (WPLEDs) based on the emissions of complex **5** were fabricated and characterized. The optimized device (device **K**) had a structure of ITO/PEDOT:PSS/PVK:OXD-7:complex **5**/TmPyPb (40 nm)/LiF (0.8 nm)/Al (100 nm) [PEDOT:PSS = poly(3,4-ethylenedioxythiophene):poly(styrene sulfonate); PVK = polyvinylcarbazole, OXD-7 = 1,3-bis[(4-*tert*-butylphenyl)-1,3,4-oxadiazolyl]phenylene, TmPyPb = 1,3,5-tri(*m*-pyrid-3-ylphenyl)benzene]. In the active layer, the weight ratio of PVK/OXD-7/complex **5** was 100:5:20. A value of 17.0 cd A^{-1} for $\eta_{L(max)}$ was obtained at 100 cd m^{-2}. In addition, the EL spectrum was stable, CIE coordinates were only slightly shifted from (0.43, 0.45) with CRI = 78 at 100 cd m^{-2} to (0.44, 0.44) with CRI = 81 at 10000 cd m^{-2} (Figure 7 and Table S16 in the Supporting Information). To the best of our knowledge, the efficiencies of device **K** with **5** as single emissive dopant are the best among the reported blend-type WPLEDs.[21]

In conclusion, a series of highly robust platinum(II) complexes **1**–**5** supported by tetradentate O^N^C^N ligands with high emission quantum yields (0.72–0.93) and high T_d (> 400 °C) have been synthesized. And high-efficiency WOLED ($\eta_{L(max)}=71.0\ cd\,A^{-1}$, $\eta_{p(max)}=55.8\ lm\,W^{-1}$, $\eta_{Ext}=16.5\%$, CIE = 0.33, 0.42, CRI = 77) and WPLED ($\eta_L=17.0\ cd\,A^{-1}$, $\eta_p=9.1\ lm\,W^{-1}$, $\eta_{Ext}=9.7\%$, CIE = 0.43, 0.45, CRI = 78) have been achieved with single emissive dopant **5**. DFT/TDDFT calculations revealed that the low-energy emission of **5** comes from excimeric excited state with a localized structure. We thus conceive that it may be possible to obtain both high- and low-energy emissions with high quantum yields by varying the substitution pattern of the tetradentate ligands without recourse to ^{3}MMLCT excited state, which is governed by Pt···Pt contacts, a factor difficult to be systematically varied or controlled.

Acknowledgements

The work described in this paper was supported by the Innovation and Technology Commission of the HKSAR Government (GHP/043/10), Research Grants Council of Hong Kong SAR (HKU 7008/09P) and Theme-Based Research Scheme (T23-713/11), National Natural Science Foundation of China/Research Grants Council Joint Research Scheme [N HKU 752/08]. This work was also supported by Guangdong Special Project of the Introduction of Innovative R&D Teams, China and Guangdong Aglaia Optoelectronic Materials Co., Ltd. The calculations in this work are supported by the Hong Kong UGC Special Equipment Grant (SEG HKU09).

Keywords: charge transfer · chelates · cyclometalation · organic light-emitting diodes · phosphoresence · platinum

[1] a) V. H. Houlding, V. M. Miskowski, *Coord. Chem. Rev.* **1991**, *111*, 145–152; b) J. A. Bailey, M. G. Hill, R. E. Marsh, V. M. Miskowski, W. P. Schaefer, H. B. Gray, *Inorg. Chem.* **1995**, *34*, 4591–4599; c) M. G. Hill, J. A. Bailey, V. M. Miskowski, H. B. Gray, *Inorg. Chem.* **1996**, *35*, 4585–4590.

[2] a) B. Ma, J. Li, P. I. Djurovich, M. Yousufuddin, R. Bau, M. E. Thompson, *J. Am. Chem. Soc.* **2005**, *127*, 28–29; b) J. A. G. Williams, *Top. Curr. Chem.* **2007**, *281*, 205–268; c) K. M.-C. Wong, V. W.-W. Yam, *Acc. Chem. Res.* **2011**, *44*, 424–434.

[3] a) H.-K. Yip, C.-M. Che, Z.-Y. Zhou, T. C. W. Mak, *J. Chem. Soc. Chem. Commun.* **1992**, 1369–1371; b) S.-W. Lai, M. C.-W. Chan, T.-C. Cheung, S.-M. Peng, C.-M. Che, *Inorg. Chem.* **1999**, *38*, 4046–4055; c) W. Lu, M. C. W. Chan, N. Zhu, C.-M. Che, C. Li, Z. Hui, *J. Am. Chem. Soc.* **2004**, *126*, 7639–7651; d) S.-W. Lai, C.-M. Che, *Top. Curr. Chem.* **2004**, *241*, 27–63.

[4] a) W. Lu, V. A. L. Roy, C.-M. Che, *Chem. Commun.* **2006**, 3972–3974; b) F. Camerel, R. Ziessel, B. Donnio, C. Bourgogne, D. Guillon, M. Schmutz, C. Iacovita, J.-P. Bucher, *Angew. Chem.* **2007**, *119*, 2713–2716; *Angew. Chem. Int. Ed.* **2007**, *46*, 2659–2662; c) M.-Y. Yuen, V. A. L. Roy, W. Lu, S. C. F. Kui, G. S. M. Tong, M.-H. So, S. S.-Y. Chui, M. Muccini, J. Q. Ning, S. J. Xu, C.-M. Che, *Angew. Chem.* **2008**, *120*, 10043–10047; *Angew. Chem. Int. Ed.* **2008**, *47*, 9895–9899; d) W. Lu, S. S.-Y. Chui, K.-M. Ng, C.-M. Che, *Angew. Chem.* **2008**, *120*, 4644–4648; *Angew. Chem. Int. Ed.* **2008**, *47*, 4568–4572; e) W. Lu, Y.-C. Law, J. Han, S. S.-Y. Chui, D.-L. Ma, N. Zhu, C.-M. Che, *Chem. Asian J.* **2008**, *3*, 59–69; f) W. Lu, Y. Chen, V. A. L. Roy, S. S.-Y. Chui, C.-M. Che, *Angew. Chem.* **2009**, *121*, 7757–7761; *Angew. Chem. Int. Ed.* **2009**, *48*, 7621–7625; g) Y. Chen, K. Li, W. Lu, S. S.-Y. Chui, C.-W. Ma, C.-M Che, *Angew. Chem.* **2009**, *121*, 10093–10097; *Angew. Chem. Int. Ed.* **2009**, *48*, 9909–9913; h) C.-M. Che, C.-F. Chow, M.-Y. Yuen, V. A. L. Roy, W. Lu, Y. Chen, S. S-Y. Chui, N. Zhu, *Chem. Sci.* **2011**, *2*, 216–220.

[5] a) I. Eryazici, C. N. Moorefield, G. R. Newkome, *Chem. Rev.* **2008**, *108*, 1834–1895; b) V. W.-W. Yam, K. M.-C. Wong, *Chem. Commun.* **2011**, *47*, 11579–11592.

[6] V. M. Miskowski, V. H. Houlding, *Inorg. Chem.* **1989**, *28*, 1529–1533.

[7] D. Kim, J.-L. Brédas, *J. Am. Chem. Soc.* **2009**, *131*, 11371–11380.

[8] B. D′Andrade, S. R. Forrest, *Chem. Phys.* **2003**, *286*, 321–335.

[9] J. Kalinowski, M. Cocchi, L. Murphy, J. A. G. Williams, V. Fattori, *Chem. Phys.* **2010**, *378*, 47–57.

[10] D. F. O'Brien, M. A. Baldo, M. E. Thompson, S. R. Forrest, *Appl. Phys. Lett.* **1999**, *74*, 442–444.

[11] Y.-Y. Lin, S.-C. Chan, M. C. W. Chan, Y.-J. Hou, N. Zhu, C.-M. Che, Y. Liu, Y. Wang, *Chem. Eur. J.* **2003**, *9*, 1263–1272.

[12] a) C.-M. Che, S.-C. Chan, H.-F. Xiang, M. C. W. Chan, Y. Liu, Y. Wang, *Chem. Commun.* **2004**, 1484–1485; b) C.-M. Che, C.-C. Kwok, S.-W. Lai, A. F. Rausch, W. J. Finkenzeller, N. Zhu, H. Yersin, *Chem. Eur. J.* **2010**, *16*, 233–247.

[13] H.-F. Xiang, S.-C. Chan, K. K.-Y. Wu, C.-M. Che, P. T. Lai, *Chem. Commun.* **2005**, 1408–1410.

[14] D. A. K. Vezzu, J. C. Deaton, J. S. Jones, L. Bartolotti, C. F. Harris, A. P. Marchetti, M. Kondakova, R. D. Pike, S. Huo, *Inorg. Chem.* **2010**, *49*, 5107–5119.

[15] K. Li, X. Guan, C.-W. Ma, W. Lu, Y. Chen, C.-M. Che, *Chem. Commun.* **2011**, *47*, 9075–9077.

[16] CCDC-830686 (**1**), 854346 (**3**), and 885383 (**5**) contain the supplementary crystallographic data for this paper. These data can be obtained free of charge from The Cambridge Crystallographic Data Centre via www.ccdc.cam.ac.uk/data_request/cif.

[17] We have used two different strategies to optimize the lowest triplet excited state: DFT and TDDFT. Both methods locate the lowest triplet excited state of **5** with similar character, namely, $^3MLCT_B$, but the latter method predicts a shorter C10–C12 distance (1.41784 Å with DFT and 1.39676 Å with TDDFT). Frequency calculations were performed on both DFT and TDDFT optimized geometries and both were found to have no imaginary frequency. This shows that the potential energy surface of $^3MLCT_B$ is rather flat while the ground state of **5** is not. Thus, we report here a range of energies for the low-energy emission for **5**.

[18] E. L. Williams, K. Haavisto, J. Li, G. E. Jabbour, *Adv. Mater.* **2007**, *19*, 197–202.

[19] X. Yang, Z. Wang, S. Madakuni, J. Li, G. E. Jabbour, *Adv. Mater.* **2008**, *20*, 2405–2409.

[20] a) J. Kalinowski, M. Cocchi, D. Virgili, V. Fattori, J. A. G. Williams, *Adv. Mater.* **2007**, *19*, 4000–4005; b) J. Kalinowski, V. Fattori, M. Cocchi, J. A. G. Williams, *Coord. Chem. Rev.* **2011**, *255*, 2401–2425.

[21] X. Yang, J. D. Froehlich, H. S. Chae, B. T. Harding, S. Li, A. Mochizuki, G. E. Jabbour, *Chem. Mater.* **2010**, *22*, 4776–4782.

Received: October 16, 2012
Published online: December 13, 2012

